



## QUALITY SURFACE ANALYSIS FOR POLARIZED GRID PLASMA NITRIDING

Mihai AXINTE, Manuela-Cristina PERJU,  
Carmen NEJNERU, Ion HOPULELE, Iulian CIMPOEȘU

"Gheorghe Asachi" Technical University from Iași  
email: mihai.axinte@gmail.com

### ABSTRACT

*For the study regarding the effect of the polarized grid a prototype plasma nitriding facility was used. A polarized grid was placed inside the working chamber, into the space between the anode and cathode, a negative polarised grid.*

*The sample used for the tests has a special configuration, provided with three different diameter holes, to highlight the hollow cathode effect on the holes near by sample areas.*

*The chemical analysis for the deposited surface layer was made.*

KEYWORDS: plasma nitriding, cathodic active screen grid, hollow cathode effect, scanning electron microscopy

### 1. Introduction

Plasma nitriding process and, in the last years, plasma nitriding assisted by glow discharge plasma are used for improving surface hardness, fatigue strength, and corrosion or wear resistance of industrial components for a wide range of different applications.

Recently, conventional plasma nitriding has been extensively used for the surface modification of different alloy steels. But, because of different problems in this technique, such as overheating of some parts due to the "hollow cathode effect" and non-uniform properties of work pieces by the "edging effect" [1], a new method of plasma nitriding, known as active screen plasma nitriding, has been developed [6–8]. Since plasma is generated also on the part and screen surface, the arcing damage and the "edge effect" can be avoided by this technique [5]. In this method, the components are surrounded by a metal screen or cage and a negative high voltage is applied to the part and to the screen,

so the term "active screen" is employed [7]. Thus, the plasma generates on the screen rather than on the component surface, and heats it up. The screen has the major role of modifying the electric field.

Active screen has a role to change the electric field between the anode and cathode in this case the influence of cathode sputtering intensity and the way is this done, "protecting" partially corner and edge areas and areas with holes, where edge effects and hollow cathode may occur [4].

### 2. Experimental conditions

#### 2.1. Sample preparation

Were used steel samples type 38CrMoAl09. The chemical composition for the used sample is presented in table 1, and it was determined using the Foundry Master spectrometer from the Department of Technologies and Equipments for Materials Processing in the Faculty Materials Science and Engineering from Iași.

Table 1. Chemical composition for 38CrMoAl09 steel

Element	Fe	C	S	Cr	Mo	Ni	Al	Cu	W	Ti
%	95.4	0.503	0.296	1.49	0.127	0.122	1.17	0.122	0.065	0.016

For the experiment we used a prototype plasma nitriding installation, built into the same department, previously mentioned. The installation is provided with a vacuum chamber, where the thermochemical

treatment takes place. The part is connected to the cathode and the chamber to the anode. In addition to the classical plasma nitriding facilities this one is provided with an active screen which encloses the

part. This screen is made by stainless steel grid, by wire with  $d=0.5\text{mm}$ , holes of  $0.5\text{mm}$  (Figure 4). This screen is connected to a DC electric, with variable

voltage, electrically insulated by the part. The screen is cylindrical with  $d=65\text{mm}$ , opened at the bottom and top.

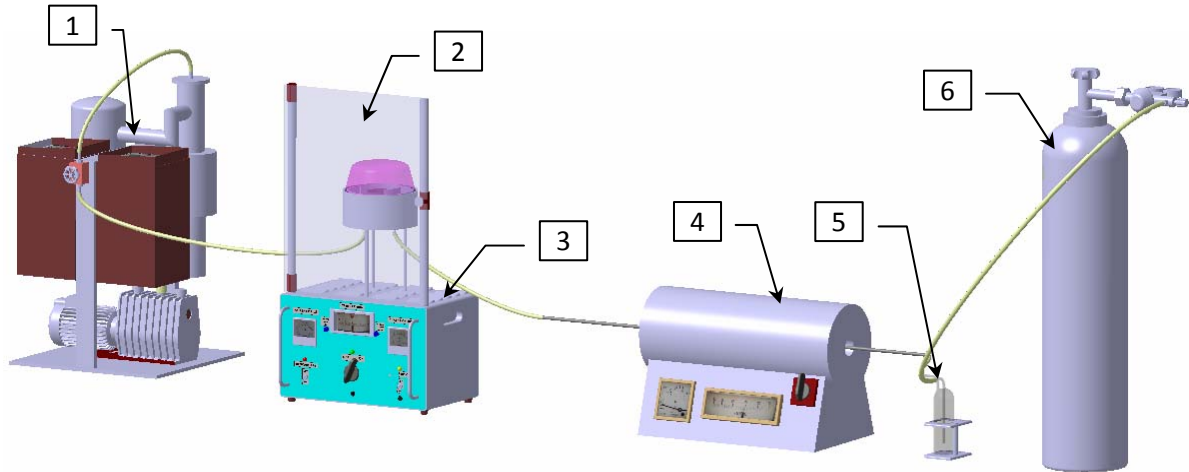


**Fig. 1.** The 3D model for the built facility: 1) flow control valve for ammonia; 2) vacuum device; 3) electric block and nitriding chamber; 4) ammonia dissociation device; 5) bubble meter; 6) tank of ammonia

To simulate the real conditions in an industrial facility, and to highlight the hollow cathode effect and the edge effect, a cylindrical shape sample with specific geometry was used.

Perpendicular to the cylinder axis, 3 holes were made into the sample part:  $d_1=3\text{mm}$ ,  $d_2=4\text{mm}$ ,  $d_3=5\text{mm}$ . The distance between the holes of the axis is  $8.75\text{mm}$  (Figure 5).

The installation contains the following main parts:

1. The discharge chamber with the vacuum system and the gas flowing system.

2. Electric installation for power and adjustments.

The discharge chamber contains the cathode which is the nitriding element, provided with a thermocouple to measure and to adjust the temperature, the voltage and the intensity discharge, [2]. Also the chamber is connected to a vacuum chamber which ensures a pressure between up to  $10^{-3}\text{Torr}$ . For washing the working chamber with nitriding agent, the ammonia gas tank is connected to the working chamber through a gas supply pipe, with the flow control capabilities (Figure 1).

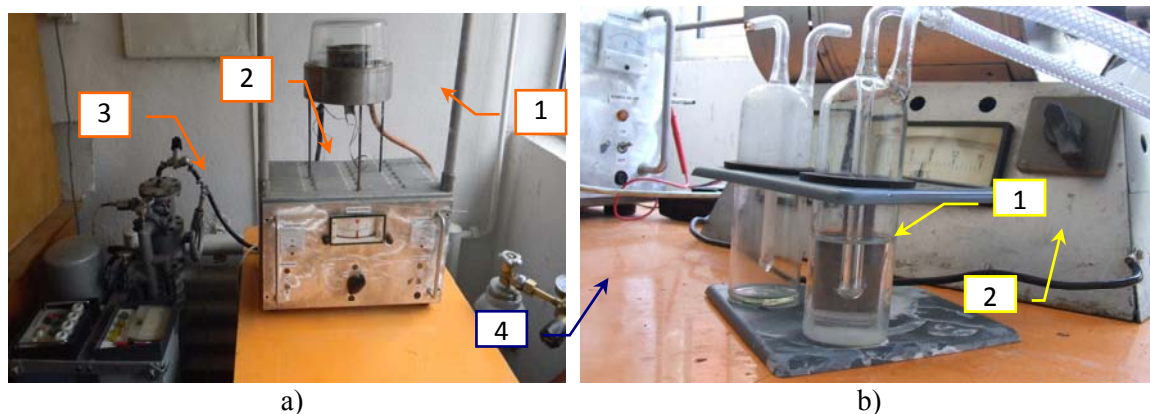


**Fig. 2.** a) Plasma nitriding installation, partial view: 1) plasma nitriding chamber; 2) electric block; 3) vacuum device; 4) tank of ammonia; b) Plasma nitriding installation detail: 1) bubble meter for gas dosage; 2) ammonia dissociation furnace

Discharge regime parameters have been stabilized to the following values: temperature  $T=500^{\circ}\text{C}$ , pressure during treatment:  $P=2\text{torr}$ ; cathode

voltage:  $U_k=468\text{V}$ ; cathode intensity  $I_k=0.18\text{A}$ ; active screen voltage  $U_g=250\text{V}$ , active screen intensity:  $I_g=0.007\text{A}$ ; treatment time:  $t=7\text{hours}$ .

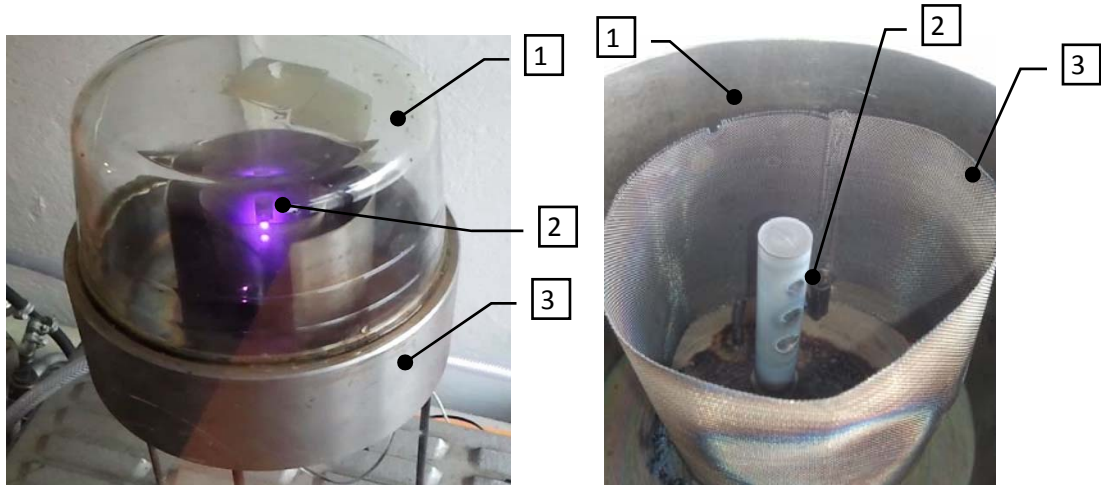


**Fig. 3.** a) Discharge halo appearance during active screen plasma nitriding: 1) sealing glass cap; 2) the halo discharge during plasma nitriding; 3) chamber floor; b) appearance of the sample after nitriding: 1) anode; 2) sample; 3) grid active screen

In this nitriding regime, the hollow cathode effect was completely removed in the small 3 mm hole, for 4 mm diameter hole the hollow cathode is fluctuating, in a transient state, being used as a condition of signaling to maintain the discharge parameters steady, not to reach the condition of occurrence of hollow cathode effect in the 3 mm hole. For the 5mm hole, the hollow cathode effect persisted permanently, as it is presented in Figure 3, where is presented a picture feature for thermo-chemical treatment regime.

After nitriding, the chamber was open, the aspect for the nitrided piece with active screen is shown in Figure 2.

### 2.2. Surface deposition

Taking into consideration the fact that the specimen studied has three holes with a different diameter and hollow cathode effect acted differently in each of the three holes, a set of micrographs were taken near each of these holes in order to observe the morphology of the deposition for each case. We observed that during ionic nitriding the hollow cathode effect is likely to occur mainly on the hole with 5 mm diameter size.

In this paper the hollow cathode effect and edge effect were studied on the proximity of 5mm diameter hole taking into account the characteristics of deposition with SEM and EDX type analyses. In figure 4 is shown the area next to the 5mm hole edge. Using the electronic scanning microscope, coupled with an EDX type QUANTAX – Bruker detector, the chemical analysis for the deposited surface layer was made.

### 3. Results and discussion

At high power magnification, 5000x, it is observed that due to the active screen, there was no problems regarding deposition. Because of this, the sputtered cathode surface is less rough than the classical treatment, resulting a uniform deposition.

A set of chemical analyses in three areas situated near the edge of the 5 mm hole was performed. The areas to perform the analysis are illustrated in Figure 5. The tables present the results obtained from the chemical analyses. Thus, in tables 2, 3 and 4 are presented the chemical composition of surface layers in area 1, 2 and 3 respectively, according to Figure 4.

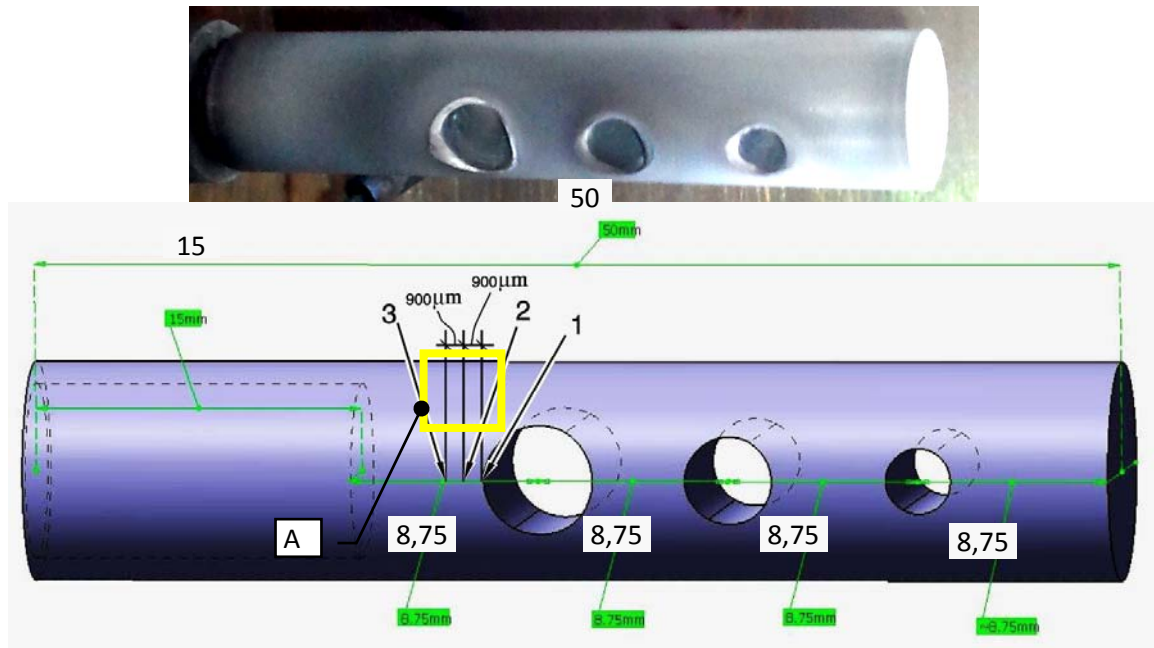


**Fig. 4.** Schematic illustration for chemical analyses areas were close to the 5mm diameter hole: 1) edge area; 2) 0.9mm away from the edge; 3) 1.8mm away from the edge; A - area of sampling images close to the 5mm hole

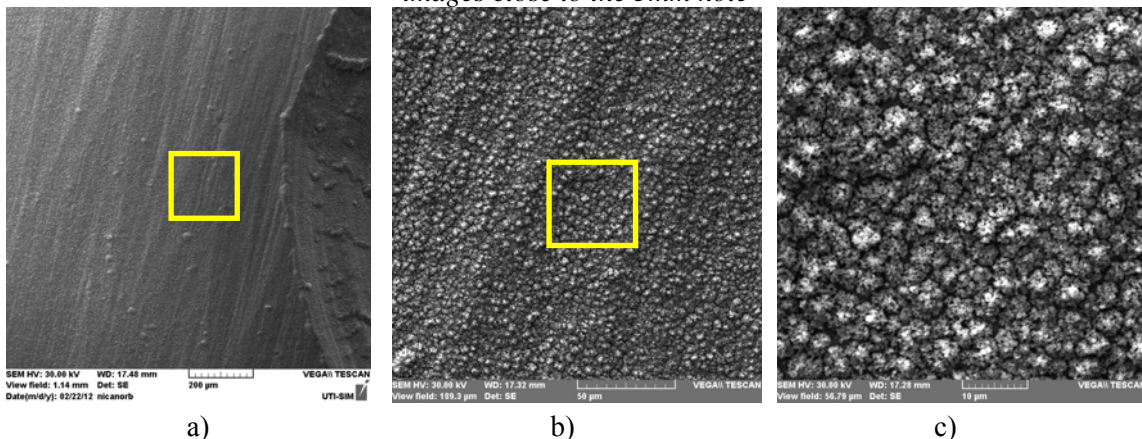


**Fig. 5.** Surface microstructures next to the 5mm hole obtained after plasma nitriding thermochemical treatment with active screen. S.E.M photographs on different scales: a) 200x; b) 1500x; c) 5000x

**Table 2.** Chemical composition of the layer in area 1, near the 5mm diameter hole

Element	Iron	Nitrogen	Oxygen	Chromium	Carbon	Aluminum	Silicon
%	Balance	7.747	7.111	1.946	0.452	1.117	0.608

**Table 3.** Chemical composition of the layer in area 2, 0.9mm near the 5mm diameter hole

Element	Iron	Nitrogen	Oxygen	Chromium	Carbon	Aluminum	Silicon
%	Balance	9.611	8.289	1.678	1.501	0.921	0.521

**Table 4.** Chemical composition of the layer in area 3, 1.8 mm near the 5mm diameter hole

Element	Iron	Nitrogen	Oxygen	Chromium	Carbon	Aluminum	Silicon
%	Balance	9.092	5.740	1.539	1.531	0.929	0.421

From THE EDX analysis, it can be seen that in zone 1, near the hole there is a lower percentage of N physico-chemical absorbed on the surface – 7.74%, compared to the points located at a specific distance from the hole wall, 9.611% N at 0.9mm in area 2, and

9.092% on the surface at 1.8mm in area 3. The following pictures are graphic representations of distributions of chemical elements in the deposited layer near the 5 mm diameter hole.

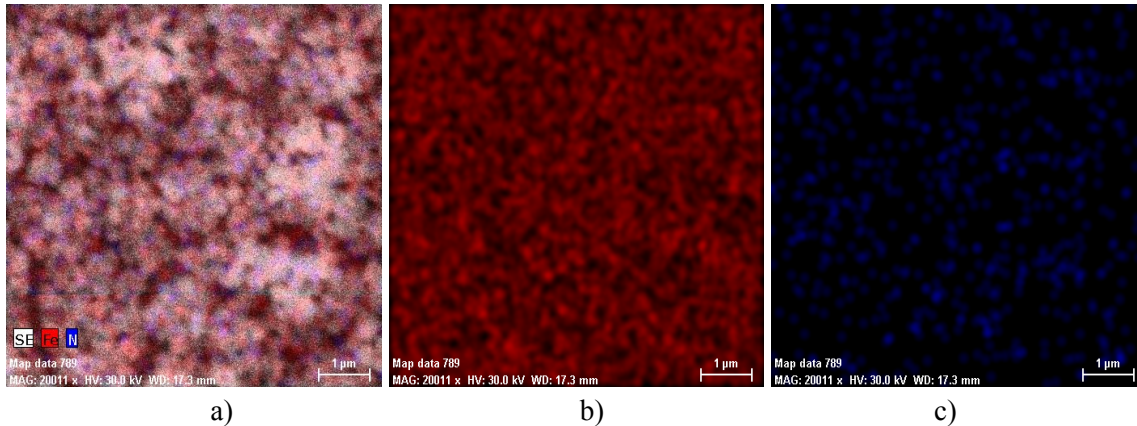


Fig. 6. Distributions of chemical elements in the deposited layer near the 5mm diameter hole:  
 a) Fe, N distribution; b) Fe distribution; c) N distribution

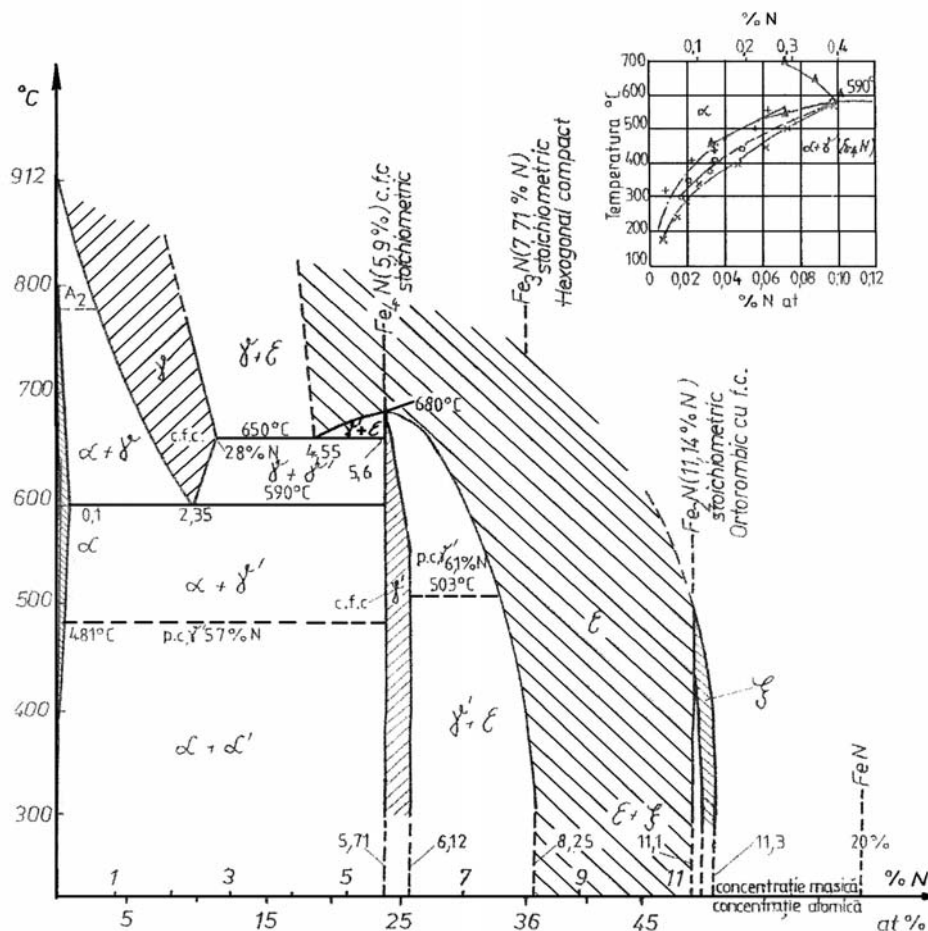


Fig. 7. Equilibrium diagram for Fe-N alloy



The study of the EDX analysis in areas 1, 2 and 3 (see tables 2, 3 and 4) shows that near the hole edge, the C and the N percent drops. This is explained by the fact that on the edge there has been a concentration of plasma (two negative glows). Also the hollow cathode effect and the edge effect are competing in that specific circular area. This effect, on classic plasma nitriding meets even stronger in edge areas, and fading color rings are present. This means a more obvious decrease in the amount of C and N, due to the temperature rising because the electrons are accelerated between the opposite surfaces of the walls [6].

If the temperature diffusion process is lower than the eutectoid transformation (591°C), on the steel surface is formed the first phase  $\alpha$  (solid solution of nitrogen in Fe $\alpha$ ), and when overcome the saturation limit will occur in order the following phases:  $\gamma'$  (nitride Fe<sub>4</sub>N) and  $\epsilon$  (solid solution based Fe<sub>3</sub>N); consequently.

As temperatures drop,  $\alpha$  and  $\epsilon$  phases decompose and precipitate the  $\gamma'$  'excess phase (Figure 7). Therefore, at room temperature, the phase sequence present in the nitrided layer (from surface to core) is the following:  $\epsilon \rightarrow \epsilon + \gamma' \rightarrow \gamma' \rightarrow \alpha + \gamma' \rightarrow \alpha$ . If nitriding is performed at a temperature above the eutectoid, example 600°C,  $\alpha$  phase is formed first and after the saturation limit of successive phases occur  $\gamma$ ,  $\gamma'$  and  $\epsilon$  phases occurs. At the diffusion temperature, the nitrided layer will consist of the following phases:  $\epsilon \rightarrow \epsilon \rightarrow \gamma' \rightarrow \gamma \rightarrow \alpha$  [6].

The slow cooling causes decomposition of  $\alpha$  and  $\epsilon$  phases, precipitates excess  $\gamma'$  phase, while the  $\gamma$  phase undergoes eutectoid transformation, creating a mechanical mixture of  $\alpha$  and  $\gamma'$ . Nitrided layer will contain the following phases at room temperature (from surface to core):  $\epsilon \rightarrow \epsilon + \gamma'$ ,  $\gamma'$ ,  $\alpha + \gamma'$  (eutectoid),  $\alpha + \gamma'$  (secondary)  $\rightarrow \alpha$ .

Note that the N absorbed on the edge in the structure is less than on the surfaces, due to the fact that the edge temperature is higher than the middle zone and can exceed the amount of 590°C, [3]. The nitrogen solubility degree in structures at T>600°C is smaller than T<590°C.

Usually diffusion is directly proportional to the thermochemical treatment temperature, but for nitrogen it is smaller at temperatures higher than 590°C and higher at temperatures smaller than this. This results in a smaller thickness of nitrided layer and diffusion layer in edge areas.

## 4. Conclusions

1. The active screen grid main result is reducing sample surface damage by an intense sputtering, comparing to the classical plasma nitriding technology. This fact is highlighted by the lowest values of the studied surface.

2. The hollow cathode effect generally occurs on the surfaces of parts at a distance less than the cathodic falling distance is decreased by the presence of the grid but not canceled, because in the nearest area to the hole, a slight decarburising is observed and also a slight decreasing nitrogen concentration in the surface layer. For the classical plasma nitriding treatment these effects are much more powerful.

3. The edge effect which is present at classical plasma nitriding treatment showed by the fading color rings on the edge area is almost canceled with this active screen grid technology.

## Acknowledgement

This paper was realised with the support of POSDRU CUANTUMDOC "DOCTORAL STUDIES FOR EUROPEAN PERFORMANCES IN RESEARCH AND INOVATION" ID79407 project funded by the European Social Found and Romanian Government.

## References

- [1]. Alves C. Jr. et al. - Nitriding of titanium disks and industrial dental implants using hollow cathode discharge, Surface & Coatings Technology 194, pp 196–202, (2005).
- [2]. Axinte M. et. al. - Facility for study heating and diffusion process, using a ionic triode in a plasma nitriding installation, Tehnomus XV, Suceava, pp. 223-228, (2009).
- [3]. Corujeira Gallo S., Dong H. - Study of active screen plasma processing conditions for carburising and nitriding austenitic stainless steel, Surface & Coatings Technology 203, pp. 3669–3675, (2009).
- [4]. Janosi S. et al. - Controlled hollow cathode effect: new possibilities for heating low-pressure furnaces, Metal Science and Heat Treatment, Vol. 46, Nos.7–8, pp. 310-316, (2004).
- [5]. Li C. X. et al. - Active screen plasma nitriding of austenitic stainless steel, Surface Engineering, Vol. 18, No. 6, pp. 453-457, (2002).
- [6]. Vermesan G., Deac V. - Procese fizico-chimice la nitrurarea ionica, Bazele tehnologice ale nitrurarii ionice, Editura Universitatii din Sibiu, pp. 26-35, Sibiu, (1992).
- [7]. S.D. de Souza, M. Kapp, M. Olzon-Dionysio, M. Campos - Influence of gas nitriding pressure on the surface properties of ASTM F138 stainless steel. Surface & Coatings Technology 204 pp. 2976–2980, (2010).
- [8]. K.J.B. Ribeiro et al. - Industrial application of AISI 4340 steels treated in cathodic cage plasma nitriding technique, Materials Science and Engineering A 479 pp 142–147, (2008).